**THE EUROPEAN
PHYSICAL JOURNAL PLUS**

Quantum speed of evolution of neutral mesons

Subhashish Banerjee[a], K. G. Paulson[b]

Indian Institute of Technology Jodhpur, Jodhpur 342011, India

Abstract We investigate the quantum-mechanical time-evolution speed limit for neutral K and B mesons, both single as well as correlated, within the framework of open quantum systems. The role of coherence–mixing, a crucial feature of the open system evolution of the underlying quantum systems (here, the mesons), on the quantum-mechanical time-evolution speed limit is studied. The impact of decoherence and CP (charge conjugation parity) symmetry violation on quantum-mechanical time-evolution speed limit is also investigated. The quantum-mechanical time-evolution speed limit increases with the evolution time for the single mesons, a signature of the underlying open system dynamics of the evolution being semi-group in nature. The evolution of the correlated mesons slows down for an evolution time of approximately one-fourth of the lifetime, after which it is sped up. An overall pattern that emerges is that correlated mesons evolve faster, as compared to their uncorrelated counterparts, suggesting that quantum correlations can speed up evolution.

1 Introduction

The theory of quantum mechanics has revolutionized our understanding of the universe at the smallest scales. One of the key features of quantum mechanics is that it allows for the existence of superposition and entanglement. Significant advancements in science and technology have been made possible by exploiting entanglement and superposition, which would be otherwise impossible. This has inspired the investigation of quantum correlations and their applications in high energy systems also, in particular, meson and neutrino systems [1–8]. The nature of spatial [9–16] and temporal [17–21] quantum correlations, quantum coherence [22], geometric phase [23–29], non-standard interactions [30], as well as the impact of decoherence in neutral meson and neutrinos, have also been studied [31–37].

Heisenberg's uncertainty principle is a fundamental concept in quantum mechanics. The uncertainty principle for position and momentum shows the impossibility of simultaneous measurement of both position and momentum precisely, but the interpretation of the energy–time uncertainty relation in this line is not so obvious. In [38], Mandelstam and Tamm (MT) showed that the energy–time uncertainty principle $\left(\Delta t \gtrsim \frac{\hbar}{\Delta E}\right)$ is a statement about the intrinsic time in which a quantum system evolves. The notion of the speed of transportation of a quantum system, the quantum-mechanical time-evolution speed limit (QMTSL), was first introduced in [39] using the geometric approach, making use of the Fubini-Study metric on the space of quantum pure states. The significance of this is that the length of any path connecting two distinguishable pure states is lower bounded by the geodesic length between them according to the Fubini-Study metric. Margolus, Levitin (ML) [40] provided a different QMTSL, which depends on the mean energy. The QMTSL for unitary dynamics, restricted to orthogonal pure states, can be made tighter by combining the MT and ML bounds as $\tau_{QSL} = \max\{\frac{\pi\hbar}{2\Delta H}, \frac{\pi\hbar}{2\langle H\rangle - E_0}\}$. τ_{QSL} refers to the minimum amount of time required for a quantum system to evolve from one state to another. It sets a fundamental limit on the speed at which quantum information can be processed or transmitted and is also connected to the stability of matter [41]. It plays a crucial role in the development of quantum technologies such as quantum computing and quantum communication. Any real system interacts with its environment, which can lead to a loss of quantum coherence. This can be taken into account by using the ideas of open quantum systems [42–44]. The extension of the QMTSL to open quantum systems [45–48] has important implications for the design and implementation of quantum information processing protocols [47]. Recently, a good amount of work has been done in this domain, its connection with resource theory, and usefulness for other technological aspects [48–54].

The treatment of unstable systems has a long history [55–65]. The study is facilitated by the use of the density matrix formalism, a view supported by work on decaying systems using dynamical semi-groups [66], where it was suggested that a unitary evolution

[a] e-mail: subhashish@iitj.ac.in

[b] e-mail: paulsonkgeorg@gmail.com (corresponding author)

of an unstable system along with its decay products is not feasible. Hence, a decaying system is intrinsically an open system, even without explicitly invoking an external environment.

In this work, we aim to investigate the role of the QMTSL in the dynamics of the decaying single and the correlated neutral mesons, K^0, B_d^0 and B_s^0. The neutral mesons exhibit the interesting feature of flavor oscillations. A study of quantum speed would thus serve to develop insight into the dynamics of flavor oscillations. Further, since mesons are decaying systems, the study also serves to bring out the features of quantum speed in the context of unstable quantum systems. Quantum coherence plays a crucial role in our understanding of evolution. Decaying meson evolution, being inherently open, leads to mixing. It would thus be meaningful to study the impact of coherence and mixing [74] on the quantum speed of the meson dynamics. Quantum correlations are the epitome of quantumness in a system and highlight the utility of its quantum nature [67–71]. An interplay between various facets of quantum correlations and the CP-symmetry (charge conjugation parity symmetry) violation in the quark sector has been actively studied [33, 72, 73]. Violation in the quark sector has been shown to be a crucial ingredient in violating a Bell inequality for entangled K-meson pairs [6]. Another fact bolstering the importance of CP symmetry violation in particle physics is the parameter $\sin 2\beta$, whose measurement was the first signal for CP violation outside the neutral kaon system and helped to establish the CKM mechanism for CP violation. Correlated neutral K^0 and B^0 mesons are obtained from the decay and subsequent hadronization of the ϕ and Υ resonances, respectively. Analysis of correlated neutral mesons from the perspective of quantum speed would thus be pertinent. The role of decoherence and CP (charge-parity) violation are also considered.

The plan of the paper is as follows. We provide information related to the QMTSL and the notion of coherence and mixing in Sect. 2. This is followed by a brief discussion of both single and correlated neutral mesons and the analytical expressions of coherence and entropy for these systems (Sect. 3). In Sect. 4, these systems' QMTSL is presented and discussed, followed by the concluding remarks in Sect. 5.

2 Preliminaries

The basic notion of the QMTSL and coherence-mixing balance are presented below.

2.1 Measures of quantum-mechanical time-evolution speed limit

Mandelstam–Tamm and Margolus–Levitin-types bound on speed limit time for an open quantum system based on the geometrical distance between the initial pure state $\rho_0 = |\psi_0\rangle\langle\psi_0|$ and final state ρ_τ, which is a tighter bound is given as [45],

$$\tau_{\mathrm{QSL}} = \max \left\{ \frac{1}{\Lambda_\tau^{\mathrm{op}}}, \frac{1}{\Lambda_\tau^{\mathrm{tr}}}, \frac{1}{\Lambda_\tau^{\mathrm{hs}}} \right\} \sin^2[\mathcal{B}], \tag{1}$$

where $\frac{1}{\Lambda_\tau^{\mathrm{op}}}, \frac{1}{\Lambda_\tau^{\mathrm{tr}}}$, and $\frac{1}{\Lambda_\tau^{\mathrm{hs}}}$ corresponds to the operator, trace, and Hilbert–Schmidt norms, respectively. Bures angle $\mathcal{B}(\rho_0, \rho_\tau) = \arccos \sqrt{\mathcal{F}(\rho_0, \rho_\tau)}$, where the Bures fidelity $\mathcal{F}(\rho_0, \rho_\tau)$ is $\left[\mathrm{tr}[\sqrt{\sqrt{\rho_0}\rho_\tau\sqrt{\rho_0}}] \right]^2$ and,

$$\Lambda_\tau^{\mathrm{op,tr,hs}} = \frac{1}{\tau} \int_0^\tau \mathrm{d}t\, ||\mathcal{L}(\rho_t)||_{\mathrm{op,tr,hs}}. \tag{2}$$

As it is known, the operators obey the following inequality $||\cdot||_{\mathrm{op}} \leq ||\cdot||_{\mathrm{hs}} \leq ||\cdot||_{\mathrm{tr}}$, as a result, we have, $1/\Lambda_\tau^{\mathrm{op}} \geq 1/\Lambda_\tau^{\mathrm{hs}} \geq 1/\Lambda_\tau^{\mathrm{tr}}$, which shows that the QMTSL, based on the operator norm of the nonunitary generator provides the tighter bound on τ_{QSL} for an actual evolution time τ.

The geometrical approach for the quantum speed limit, as discussed here, relies on the geodesic distance between any two points is the shortest possible lengths connecting them. This idea was brought out in [39] in the context of an extension of the MT bound to time-dependent Hamiltonians on the space of quantum pure states. The geometric quantum speed limits are not sensitive to instantaneous speed; the problem is resolved by the action τ_{QSL} [50]. In [48], an important observation was highlighted in that there exist an infinite family of contractive Riemannian metrics on the set of density matrices, which could serve as a geometric quantifier of distinguishability between the states, giving rise to a corresponding quantum speed limit (QSL). In particular, the role of the Wigner–Yanase skew information metric for mixed states was brought out.

2.2 Coherence and mixing

Quantum coherence, a quantum resource, is a significant characteristic arising from the superposition of states. Quantification of quantum coherence is dependent on the reference basis considered. Different measures are adopted to quantify the coherence of quantum states. Here, we use the l_1 norm measure of quantum coherence, defined for a state ρ and the reference basis $\{|i\rangle\}$

$$C_{l1}(\rho) = \sum_{i \neq j} |\rho_{i,j}|. \tag{3}$$

We have $\rho_{ij} = \langle i|\rho|j\rangle$.

A quantum system's inescapable interaction with its surroundings results in the loss of purity. Linear entropy quantifies the mixedness of quantum states due to, for example, their environment. For a general d-dimensional state, linear entropy is defined as

$$S_L(\rho) = \frac{d}{d-1}(1 - \text{Tr}\rho^2). \tag{4}$$

For a mixed state $0 < S_L(\rho) \le 1$. Trade-off between quantum coherence and mixedness (M_{Cl}) for a quantum state ρ is given by the inequality [74, 75]

$$S_L(\rho) + \frac{C_{l1}^2}{(d-1)^2} \le 1. \tag{5}$$

For a maximally coherent mixed state, the above quantity will equal 1.

3 Neutral mesons

Open quantum system formalism can be made use of to analyze the decay of unstable quantum systems. We consider single and correlated B^0 (K^0) neutral meson systems. Decoherence, which is due to the decaying nature of the system, is modeled here by a single phenomenological parameter [34] which represents the interaction between the one-particle system and its environment. The the environment could be attributed to quantum gravity effects [76, 77] or due to the detector background itself. Apart from decoherence, we also consider the effects of CP violation.

The experiments on the $B_0(K_0)$ meson systems involve the determination of their flavor at the time of production or decay, which is achieved by analyzing the flavor-specific decays. The charge of the final state lepton in the semileptonic decays of a neutral meson usually determines the flavor of that meson at the time of decay. This is a consequence of the $\Delta B = \Delta Q$ rule for the semileptonic decays of B mesons and is usually assumed in experiments. The process of determination of the initial flavor of a neutral meson is called tagging. This is achieved by making use of the rule of the associated production. The mesons are produced either by strong or electromagnetic interactions; hence, a quark is always produced in association with its anti-quark, as the flavor is conserved in these interactions. If two entangled neutral mesons are produced, then detecting the flavor-specific final state of one meson at a particular time determines the flavor of that meson as well as the other meson at that time. The oscillation probability of the tagged meson is then determined by identifying its final flavor-specific state.

3.1 Single neutral mesons

Here, we discuss the time decay of B^0 (K^0) mesons. The Hilbert space for the decaying meson system is $\mathcal{H}_{B^0(K^0)} \oplus \mathcal{H}_0$, where $\mathcal{H}_0$ is for vacuum state $|0\rangle$ to incorporate the decay in this system. The orthonormal spanning vectors for B^0 meson system are

$$|B^0\rangle = \begin{pmatrix} 1 \\ 0 \\ 0 \end{pmatrix}, |\bar{B}^0\rangle = \begin{pmatrix} 0 \\ 1 \\ 0 \end{pmatrix}, |0\rangle = \begin{pmatrix} 0 \\ 0 \\ 1 \end{pmatrix}. \tag{6}$$

Here B^0 stands for B_d^0 (B_s^0) mesons. Further, $|B^0\rangle$, $|\bar{B}^0\rangle$ stand for the flavor eigenstates. Similar basis vectors span the decaying K^0 meson as well. The time evolution is given by a family of completely positive trace-preserving maps forming a one-parameter dynamical semi-group and is characterized by the operator-sum representation

$$\rho(t) = \sum_i K_i(t)\rho_0 K_i^\dagger(t). \tag{7}$$

The Kraus operators in Eq. (7) can be seen in, for example, Ref. [18]. The time evolution is given by a one-parameter dynamical semi-group. Using this, for example, on a meson initially in the state $\rho_{B^0}(0) = |B^0\rangle\langle B^0|$, the evolved state $\rho_{B^0}(t)$ is given by

$$\rho_{B^0}(t) = \frac{1}{2}e^{-\Gamma t}\begin{pmatrix} \cosh\left(\frac{\Delta\Gamma t}{2}\right) + e^{-\lambda t}\cos(\Delta m\, t) & \left(\frac{q}{p}\right)^*\left(-\sin(\Delta m\, t) - i\, e^{-\lambda t}\sin(\Delta m\, t)\right) & 0 \\ \left(\frac{q}{p}\right)\left(-\sin(\Delta m\, t) + i\, e^{-\lambda t}\sin(\Delta m\, t)\right) & |\frac{q}{p}|^2\cosh\left(\frac{\Delta\Gamma t}{2}\right) - e^{-\lambda t}\cos(\Delta m\, t) & 0 \\ 0 & 0 & 2\left(e^{\Gamma t} - \left(1 + \left|\frac{q}{p}\right|^2\right)\cosh\left(\frac{\Delta\Gamma t}{2}\right)\right) \end{pmatrix}. \tag{8}$$

Here $\Delta\Gamma = \frac{\Gamma_L - \Gamma_H}{2}$ is the difference in the decay width of light, and heavy mesons, $\Gamma = \frac{\Gamma_L + \Gamma_H}{2}$ is the average decay width, $\Delta m = \frac{m_L - m_H}{2}$ and $m = \frac{m_L + m_H}{2}$ with m_L and m_H being the masses of the light and heavy mesons, respectively. Also, λ corresponds to the decoherence parameter. With the suitable change in notation, the same holds for the K^0 meson as well. Here p and q are the coefficients connecting the mass eigenstates $\{|B_L\rangle, |B_H\rangle\}$ to the flavor eigenstates $\{|B^0\rangle, |\bar{B}^0\rangle\}$ and are due to CP violation in the flavor oscillations. In particular, $|B_L\rangle = p|B^0\rangle + q|\bar{B}^0\rangle$, $|B_H\rangle = p|B^0\rangle - q\bar{B}^0\rangle$, with $|p|^2 + |q|^2 = 1$.

The linear entropy and coherence, without CP-violation (for ease in analysis), can be obtained by using Eq. (8) (without the *CP* violating terms) in Eqs. (4) and (3), respectively and are

$$S_L(\rho_{B^0}(t)) = \frac{3}{4}e^{-2(\Gamma+\lambda)t}\left(4e^{(\Gamma+2\lambda)t}\cosh\left(\frac{\Delta\Gamma t}{2}\right) - 2e^{2\lambda t}\cosh(\Delta\Gamma t) - e^{2\lambda t} - 1\right) \tag{9}$$

$$\text{Cl}_1(\rho_{B^0}(t)) = \frac{1}{2}e^{-\Gamma t}\left(|ie^{\lambda t}\sin(\Delta\text{m}\,t) - \sinh\left(\frac{\Delta\Gamma t}{2}\right)| + |i\,e^{\lambda t}\sin(\Delta\text{m}\,t) + \sinh\left(\frac{\Delta\Gamma t}{2}\right)|\right). \tag{10}$$

3.2 Correlated mesons

The initial flavor-space correlated neutral meson state of the $M\bar{M}$ meson system ($M = K^0, B_d^0, B_s^0$) is

$$|\psi\rangle = \frac{1}{\sqrt{2}}\left(|M\bar{M}\rangle - |\bar{M}M\rangle\right). \tag{11}$$

For the B^0 meson, this happens due to the decay of the Υ resonance followed by hadronization into a $B^0\bar{B}^0$ pair. The same holds for the K^0 meson, with the Υ being replaced by the ϕ meson. By projecting onto the appropriate Hilbert space [33, 34], the dynamics can be shown to evolve the state (11) to

$$\rho(t) = \chi\begin{pmatrix} |s|^4 a_- & 0 & 0 & -s^2 a_- \\ 0 & a_+ & -a_+ & 0 \\ 0 & -a_+ & a_+ & 0 \\ -s^{*2}a_- & 0 & 0 & a_- \end{pmatrix}, \tag{12}$$

where $a_\pm = (e^{2\lambda t} \pm 1)(1 \pm \delta_L)$, $\chi = \frac{(1-\delta_L)}{4(e^{2\lambda t} - \delta_L^2)}$, $\delta_L = \frac{2\text{Re}(\epsilon)}{1+|\epsilon|^2}$ and $s = \frac{1+\epsilon}{1-\epsilon}$. Here ϵ is a small CP-violating parameter and is of order $\sim 10^{-3}$ for K^0 mesons and $\sim 10^{-5}$ for $B_{d,s}^0$ mesons while λ is the decoherence parameter.

Using Eq. (12) in Eq. (4), the linear entropy of the time-dependent correlated neutral meson state can be shown to be

$$S_L(\rho) = \frac{4}{3}P_s\left(1 - \chi(4a_+^2 + a_-^2(1 + s^4)^2)\right). \tag{13}$$

Also, the l_1 norm of coherence is obtained by using Eq. (12) in Eq. (3) as

$$C_{l1}(\rho) = 2P_s(|\chi a_+| + |\chi a_- s^2|), \tag{14}$$

where the survival probability $P_s = e^{-2\Gamma t}\frac{(1-\delta_L^2 e^{-2\lambda t})}{1-\delta_L^2}$, and Γ is the meson decay width.

## 4 Results and discussions: quantum-mechanical time-evolution speed limit

Figures 1, 2 and 3 depict τ_{QSL} Eq. (1) for neutral K^0, B_d^0 and B_s^0 mesons, along with their anti-particles, plotted with respect to the evolution time τ. Both τ_{QSL} and τ are made dimensionless by scaling with respect to the lifetime of the corresponding mesons. This is pertinent as the mesons are decaying systems and would have ceased to exist after their corresponding lifetime. Generally, the actual time required for a quantum system to evolve from one state to another will be longer than the QMTSL, which is evident from the figures. It is clear from Fig. 3 the τ_{QSL} for the decay of B_s^0 is much less than its lifetime compared to other mesons. The figures
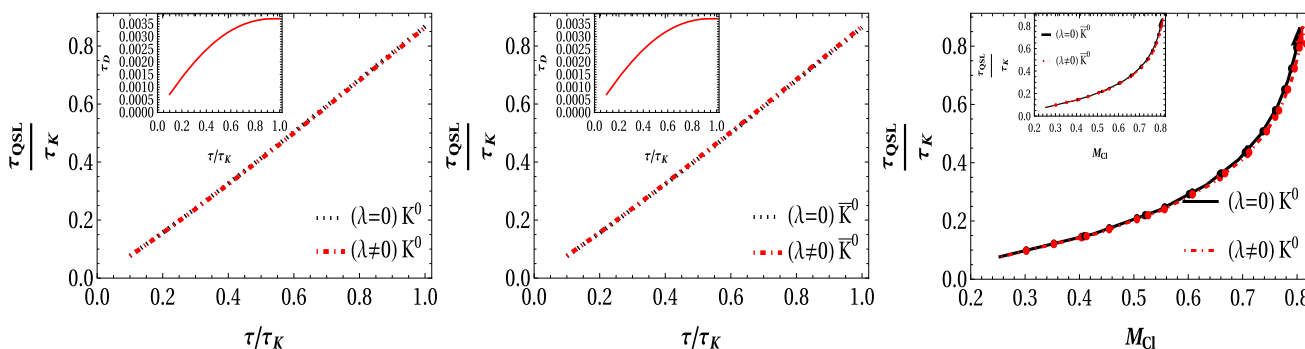
Fig. 1 QMTSL in terms of Bures measure for the decay of the K^0 and $\bar{K}^0$ meson system with and without decoherence effects (left and central subplots, respectively). For the K^0 meson system, the mean lifetime is $\tau_K = 1.7889 \times 10^{-10}s$, $\Gamma = 5.59 \times 10^9 s^{-1}$, $\Delta\Gamma = 1.1174 \times 10^{10}s^{-1}$, $\Delta m = 5.302 \times 10^9\,s^{-1}$, $m = 7.532 \times 10^{23}s^{-1}$, $\lambda = 2.0 \times 10^8\,s^{-1}$. The insets of the plots highlight the difference caused by taking decoherence, parameterized by λ, into account. The impact of the coherence-mixedness trade-off on QMTSL is also shown (right subplot)
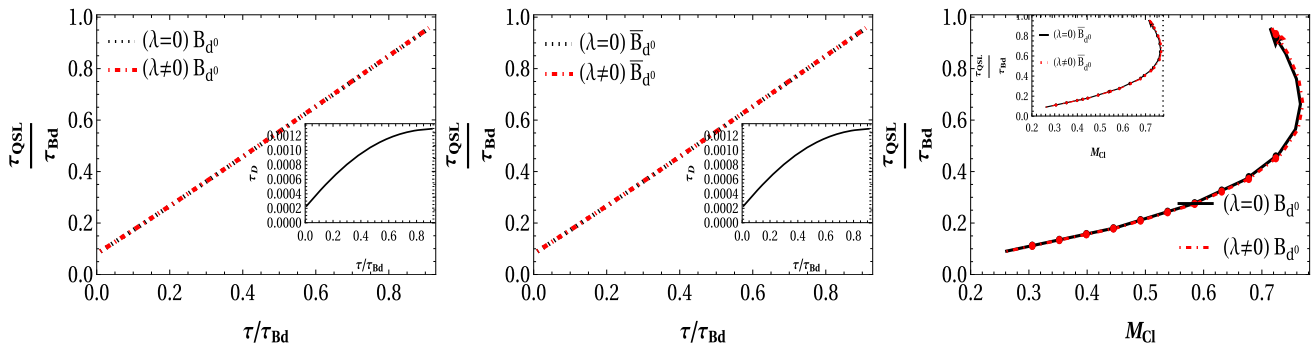
Fig. 2 QMTSL in terms of Bures measure for the decay of the B_d^0 and $\bar{B}_d^0$ meson system with and without decoherence effects (left and central subplots, respectively). For the B_d^0 meson system, the mean lifetime is $\tau_{B_d} = 1.518 \times 10^{-12}s$, $\Gamma = 6.58 \times 10^1 1 s^{-1}$, $\Delta\Gamma = 0 s^{-1}$, $\Delta m = 0.5064 \times 10^1 2 s^{-1}$, $m = 7.9917 \times 10^{24} s^{-1}$, $\lambda = 0.012 \times 10^{12} s^{-1}$. The inset of the plots highlights the difference caused by taking decoherence, parameterized by λ, into account. The impact of the coherence-mixedness trade-off on QMTSL is also shown (right subplot)
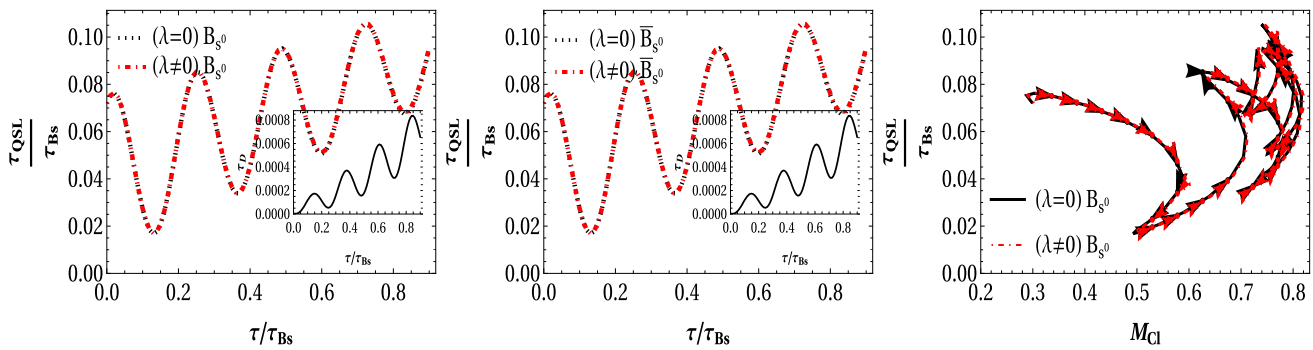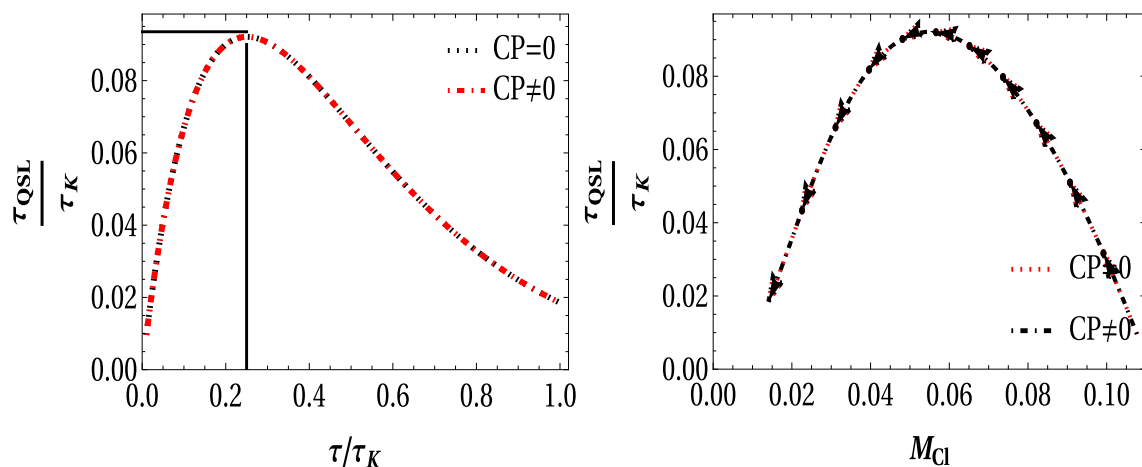

Fig. 3 QMTSL in terms of Bures measure for the decay of the B_s^0 and $\bar{B}_s^0$ meson system with and without decoherence effects (left and central subplots, respectively). For the B_s^0 meson system, the mean lifetime is $\tau_{B_s} = 1.509 \times 10^{-12} s$, $\Gamma = 0.6645 \times 10^{12} s^{-1}$, $\Delta\Gamma = 0.086 \times 10^{12} s^{-1}$, $\Delta m = 17.757 \times 10^{12} s^{-1}$, $m = 8.123 \times 10^{24} s^{-1}$, $\lambda = 0.012 \times 10^{12} s^{-1}$. The inset of the plots highlights the difference caused by taking decoherence, parameterized by λ, into account. The impact of the coherence-mixedness trade-off on QMTSL is also shown (right subplot)

Fig. 4 Difference in QMTSL for the decoherence-free evolution of K^0 and $B_{d/s}^0$ mesons
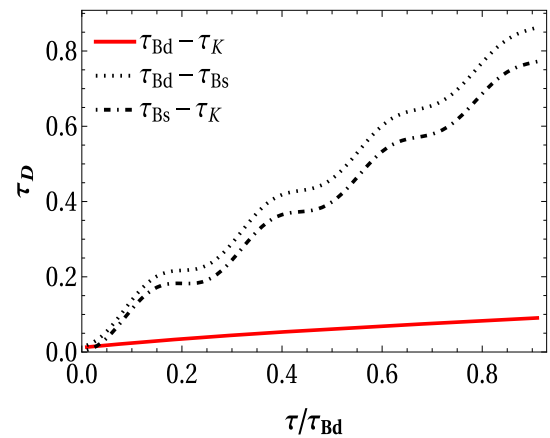
also bring out the effect of coherence and mixing, brought by the quantity M_{cl} Eq. (5), on the τ_{QSL}. As observed, the τ_{QSL} and M_{cl} are not able to distinguish between the mesons and their anti-particles, denoted by $\bar{K}^0$, $\bar{B}_d^0$ and $\bar{B}_s^0$. The insets of the plots highlight the difference caused by taking decoherence, parameterized by λ, into account. This can be seen to be of the order 10^{-3} for K^0 and B_d^0 mesons, and of the order of 10^{-4} for B_s^0 mesons. The QMTSL increases with the evolution time τ for K^0 and B_d^0 mesons. This is a signature of the underlying semi-group nature of the evolution [43]. It is consistent with the corresponding behavior under other Markovian evolutions [52] generated by a quantum dynamical semi-group [42, 44]. Different from the K^0 and B_d^0 mesons, the τ_{QSL} for B_s^0 mesons exhibit a wiggling pattern, which could be attributed to the parameter values it takes. This is in accord with a similar behavior seen for the Leggett–Garg quantity for B_s^0 mesons [18]. The mass term Δm for B_s^0 meson, which plays the role of frequency, is more than 35 times the corresponding value for the B_d^0 meson. This would account for the difference in the
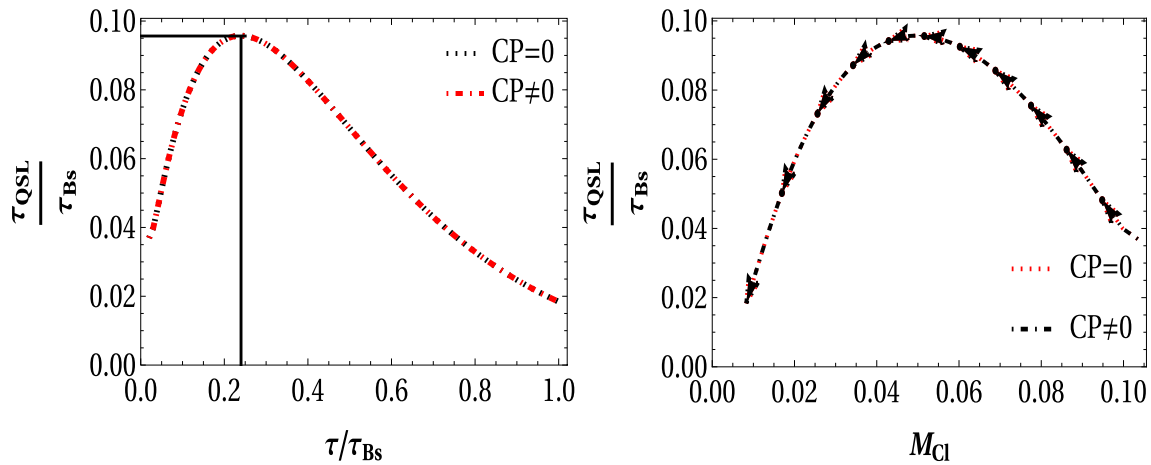
Fig. 5 τ_{QSL} in terms of Bures measure for the decay of the correlated K^0 meson system (left subplot), the mean lifetime is $\tau_{K^0} = 1.7889 \times 10^{-10} s$, $\Gamma = 5.59 \times 10^9 \, s^{-1}$, $\Delta\Gamma = 1.1174 \times 10^{10} s^{-1}$, $\Delta m = 5.302 \times 10^9 \, s^{-1}$, $m = 7.532 \times 10^{23} s^{-1}$, $\lambda = 2.0 \times 10^8 s^{-1}$. The impact of the coherence-mixedness trade-off on QMTSL is given in the right subplot
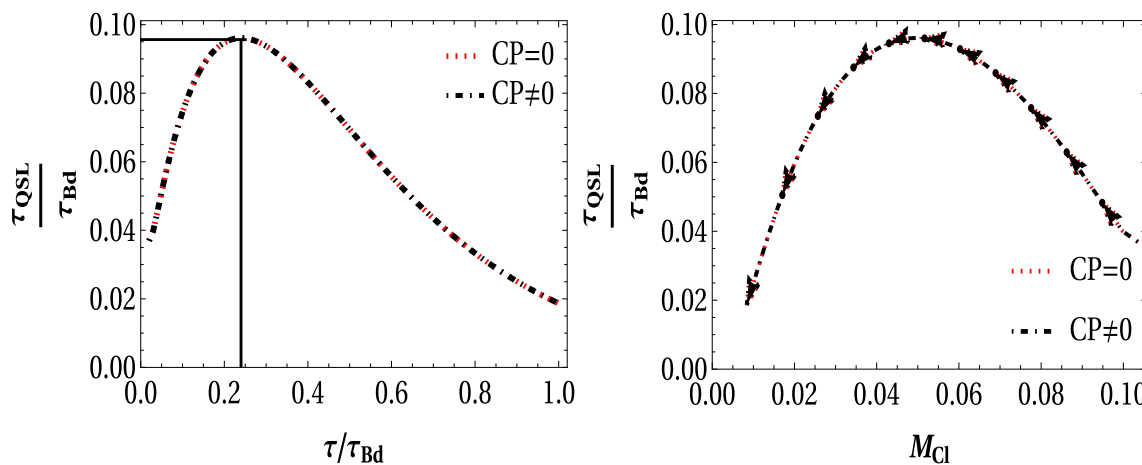
Fig. 6 QMTSL in terms of Bures measure for the decay of the correlated B_d^0 meson (left subplot), the mean lifetime is $\tau_{B_d^0} = 1.518 \times 10^{-12} s$, $\Gamma = 6.58 \times 10^{11} s^{-1}$, $\Delta\Gamma = 0 \, s^{-1}$, $\Delta m = 0.5064 \times 10^{12} s^{-1}$, $m = 7.9917 \times 10^{24} s^{-1}$, $\lambda = 0.012 \times 10^{12} s^{-1}$. The impact of the coherence-mixedness trade-off on τ_{QSl} is given in the right subplot

τ_{QSL} between the B_d^0 and the B_s^0 mesons. Figure 4 brings out the difference in QMTSL for the evolution of K^0 and $B_{d/s}^0$ mesons, with respect to evolution time τ, scaled with the lifetime of the B_d^0 meson, in the absence of decoherence. The wiggle in the curves showing the difference with the B_s^0 meson can be attributed to the above-mentioned feature of these mesons.

From Figs. 5, 6 and 7, for correlated mesons under decoherence, it can be seen that as the evolution time increases to around 0.24 τ_{lifetime}, τ_{QSL} increases, and then falls. This implies that for an evolution time of up to approximately $1/4^{\text{th}}$ of the lifetime, the evolution of correlated mesons slows down, and beyond this, as it decays, the evolution is sped up. This is consistent with the behavior of coherence-mixing balance depicted in the right panel of the figures. Here, it can be seen that, following the direction indicated by the arrows, as the M_{cl} quantity decreases, τ_{QSL} first increases and then falls. The difference in speed limit (τ_D) of evolution for different correlated mesons with respect to evolution time τ, taking decoherence into account, and scaled with the lifetime of the B_d^0 meson, are depicted in Fig. 8. These curves highlight that τ_D for B_d^0, K^0 and B_s^0, K^0 are of the order 10^{-3}, whereas for B_d^0, B_s^0, it is negligible. This difference approaches zero very quickly, within the B_d^0 meson lifetime. We also observe that the maximum speed limit time for correlated mesons is lesser than that for single mesons. This shows that correlated mesons evolve faster than single uncorrelated mesons. This is consistent with observations made in different systems that quantum correlations can speed up the evolution, see for example [54]. Further, the impact of CP violation on the dynamics of τ_{QSL} is negligible for the mesons studied.

Fig. 7 τ_{QSL} in terms of Bures measure for the decay of the correlated B_s^0 meson (left subplot), the mean lifetime is $\tau_{B_s^0} = 1.509 \times 10^{-12}s$, $\Gamma = 0.6645 \times 10^{12}s^{-1}$, $\Delta\Gamma = 0.086 \times 10^{12}s^{-1}$, $\Delta m = 17.757 \times 10^{12}s^{-1}$, $m = 8.123 \times 10^{24}s^{-1}$, $\lambda = 0.012 \times 10^{12}s^{-1}$. The impact of the coherence-mixedness trade-off on τ_{QSl} is given in the right subplot

Fig. 8 Difference in the minimum time required for the evolution of correlated K^0, B_d^0 and B_s^0 mesons, with decoherence
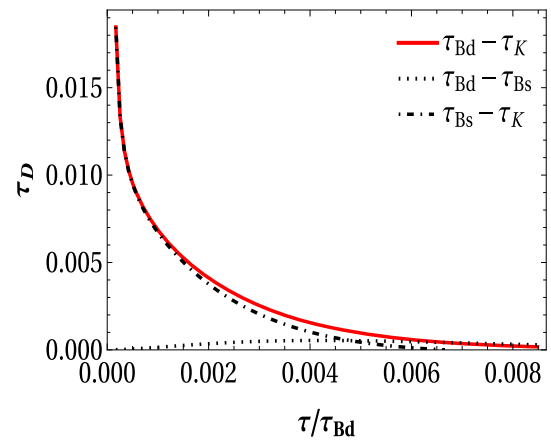
5 Conclusion

In this work, we investigated the quantum-mechanical time-evolution speed limit (QMTSL) in neutral K and B mesons, both single as well as correlated, within the framework of open quantum systems. The aim was to better understand the dynamics of these unstable subatomic systems by investigating the impact of decoherence and CP violation on the QMTSL. The impact of decoherence is seen to be minimal. The coherence–mixing, a crucial feature of the open system evolution of the underlying quantum systems (here, the neutral mesons), has an important influence on the QMTSL. Both the QMTSL and coherence–mixing balance are not able to distinguish single neutral mesons and their anti-particles.

The results showed that for single mesons, the QMTSL increased with the evolution time, which is consistent with the semi-group nature of the evolution. However, for correlated mesons, the evolution slowed down for a quarter of the meson's lifetime and then sped up, reflecting the balance between decoherence and quantum correlations in the evolution. The difference in speed limit τ_D of evolution for correlated B_d^0, K^0 and B_s^0, K^0 were seen to be of the same order, whereas they were negligible for B_s^0, K^0. The results also showed that correlated mesons evolve faster than single, uncorrelated mesons, suggesting that quantum correlations can speed up evolution.

Data Availability Statement The manuscript has no associated data.

References

1. A. Bramon, G. Garbarino, Phys. Rev. Lett. **88**, 040403 (2002)
2. A. Bramon, G. Garbarino, Phys. Rev. Lett. **89**, 160401 (2002)
3. R.A. Bertlmann, K. Durstberger, B.C. Hiesmayr, Phys. Rev. A **68**, 012111 (2003)
4. A. Bramon, G. Garbarino, B.C. Hiesmayr, Phys. Rev. A **69**, 062111 (2004)
5. B.C. Hiesmayr, Eur. Phys. J. C **50**, 73 (2007)
6. A. Go et al., Belle collaboration. Phys. Rev. Lett. **99**, 131802 (2007)
7. G. Amelino-Camelia, F. Archilli, D. Babusci, D. Badoni, G. Bencivenni, J. Bernabeu, R.A. Bertlmann, D.R. Boito et al., Eur. Phys. J. C **68**, 619 (2010)
8. B.C. Hiesmayr, A. Di Domenico, C. Curceanu, A. Gabriel, M. Huber, J.A. Larsson, P. Moskal, Eur. Phys. J. C **72**, 1856 (2012)
9. A. Bramon, R. Escribano, G. Garbarino, A review of Bell inequality tests with neutral kaons, in *Handbook on Neutral Kaon Interferometry at a Φ-factory*. ed. by A. Di (XLIII, Domenico, 2007), pp.217–254
10. M. Blasone, F. DellAnno, S. De Siena, F. Illuminati, Euro. Phys. Lett. **85**, 50002 (2009)
11. S. Banerjee, A.K. Alok, R. Srikanth, B.C. Hiesmayr, Eur. Phys. J. C **75**(10), 487 (2015)
12. A.K. Alok, S. Banerjee, S.U. Sankar, Nucl. Phys. B **909**, 65 (2016)
13. B. Kerbikov, Nucl. Phys. A **975**, 59 (2018)
14. M. Richter-Laskowska, M. Lobejko, J. Dajka, New J. Phys. **20**, 063040 (2018)
15. K. Dixit, A.K. Alok, S. Banerjee, Eur. Phy. J. C **78**, 914 (2018)
16. K. Dixit, J. Naikoo, B. Mukhopadhyay, S. Banerjee, Phys. Rev. D **100**, 055021 (2019)
17. J. Naikoo, A. K. Alok, S. Banerjee, S. Uma Sankar, G. Guarnieri, C. Schultze, B. C. Hiesmayr, Nucl. Phys. B **951**, 114872 (2020)
18. J. Naikoo, A.K. Alok, S. Banerjee, Phys. Rev. D **97**, 053008 (2018)
19. J. Naikoo, S. Banerjee, Eur. Phys. J. C **78**, 602 (2018)
20. J. Naikoo, A. K. Alok, S. Banerjee, S. Uma Sankar, Phys. Rev. D **99**, 095001 (2019)
21. J. Naikoo, S. Kumari, S. Banerjee, A.K. Pan, J. Phys. G: Nucl. Part. Phys. **47**, 095004 (2020)
22. K. Dixit, J. Naikoo, S. Banerjee, A.K. Alok, Eur. Phys. J. C **79**, 96 (2019)
23. K. Dixit, S. Banerjee, A.K. Alok, D. Kumar, J. Phys. G **45**(8), 085002 (2018)
24. B. Mukhopadhyay, S.K. Ganguly, Universe **6**, 160 (2020)
25. P. Mehta, Phys. Rev. D **79**, 096013 (2009)
26. J. Dajka, J. Syska, J. Luczka, Phys. Rev. D **83**, 097302 (2011)
27. A. Capolupo, S.M. Giampaolo, B.C. Hiesmayr, G. Vitiello, Phys. Lett. B **780**, 216 (2018)
28. L. Johns, G.M. Fuller, Phys. Rev. D **95**(4), 043003 (2017)
29. J. Lu, Phys. Lett. B **818**, 136376 (2021)
30. B. Yadav, T. Sarkar, K. Dixit, A.K. Alok, Eur. Phys. J. C **82**, 446 (2022)
31. J.R. Ellis, N.E. Mavromatos, D.V. Nanopoulos, Phys. Lett. B **293**, 37 (1992)
32. A.K. Alok, S. Banerjee, Phys. Rev. D **88**, 094013 (2013)
33. Subhashish. Banerjee, Ashutosh Kumar. Alok, Richard. MacKenzie, Eur. Phys. J. Plus 131, 5 (2016)
34. A. K. Alok, S. Banerjee, S. Uma Sankar, Phys. Lett. B **94**, 749 (2015)
35. J.R. Ellis, J.S. Hagelin, D.V. Nanopoulos, M. Srednicki, Nucl. Phys. B **241**, 381 (1984)
36. T. Banks, L. Susskind, M.E. Peskin, Nucl. Phys. B **244**, 125 (1984)
37. N. Mavromatos, S. Sarkar, Phys. Rev. D **72**, 065016 (2005)
38. L. Mandelstam, I. Tamm, J. Phys. **9**, 249 (1945)
39. J. Anandan, Y. Aharonov, Phys. Rev. Lett. **65**, 1697 (1990)
40. N. Margolus, L.B. Levitin, Phys. D: Nonlinear Phenom. **120**, 188 (1998)
41. Srishty Aggarwal, Subhashish Banerjee, Arindam Ghosh, Banibrata Mukhopadhyay, New J. Phys. **24**, 085001 (2022)
42. H.P. Breuer, F. Petruccione, *The Theory of Open Quantum Systems* (Oxford University Press, Great Clarendon Street, 2002)
43. P. Caban, J. Rembieliński, K.A. Smoliński, Z. Walczak, Phys. Rev. A **72**, 032106 (2005)
44. S. Banerjee, *Open Quantum Systems: Dynamics of Nonclassical Evolution* (Springer, Berlin, 2018)
45. S. Deffner, E. Lutz, Phys. Rev. Lett. **111**, 010402 (2013)
46. A. del Campo, I.L. Egusquiza, M.B. Plenio, S.F. Huelga, Phys. Rev. Lett. **110**, 050403 (2013)
47. S. Deffner, S. Campbell, J. Phys. A: Math. Theor. **50**, 453001 (2017)
48. D.P. Pires, M. Cianciaruso, L.C. Céleri, G. Adesso, D.O. Soares-Pinto, Phys. Rev. X **6**(2), 021031 (2016)
49. R. Baruah, K.G. Paulson, S. Banerjee, Annalen der Physik **535**, 2200199 (2022)
50. Eoin O'Connor, Giacomo Guarnieri, Steve Campbell, Phys. Rev. A **103**, 022210 (2021)
51. Y.B. Wei, J. Zou, Z.M. Wang, B. Shao, Sci. Rep. **6**, 19308 (2016)
52. K.G. Paulson, E. Panwar, S. Banerjee, R. Srikanth, Quantum Inf. Process. **20**, 141 (2021)
53. K.G. Paulson, S. Banerjee, J. Phys. A: Math. Theor. **55**(50), 505302 (2022)
54. D. Tiwari, K. G. Paulson, S. Banerjee, Annalen der Physik, 2200452 (2023)
55. V. Weisskopf, E.P. Wigner, Z. Phys. **63**, 54 (1930)
56. R.E. Peierls, Proc. R. Soc. Lond. **253A**, 16 (1960)
57. L. Khalfin, Sov. Phys. JETP **6**, 1053 (1958)
58. L. Khalfin, Sov. JETP Lett. **8**, 65 (1968)
59. T. Petrosky, I. Prigogine, Proc. Nat. Acad. Sci. U. S. A. **93**, 9393 (1993)
60. E. C. G. Sudarshan, Charles B. Chiu, G. Bhamathi, *Advances in Chemical Physics XCIX*, Wiley, Hoboken, pp. 121-210, (1997)
61. J.R. Ellis, N.E. Mavromatos, D.V. Nanopoulos, Phys. Lett. B **293**, 142 (1992)
62. P. Huet, M.E. Peskin, Nucl. Phys. B **434**, 3 (1995)
63. F. Benatti, R. Floreanini, R. Romano, Nucl. Phys. B **602**, 541 (2001)
64. K. Urbanowski, Open Syst. Inf. Dyn. **20**, 1340008 (2013)
65. M. Fabbrichesi, R. Floreanini, G. Panizzo, Phys. Rev. Lett. **127**, 161801 (2021)
66. A. Weron, A.K. Rajagopal, K. Weron, Phys. Rev. A **31**, 1736 (1985)
67. R. Horodecki, P. Horodecki, M. Horodecki, K. Horodecki, Rev. Mod. Phys. **81**, 865 (2009)
68. K. Modi, A. Brodutch, H. Cable, T. Paterek, V. Vedral, Rev. Mod. Phys. **84**, 1655 (2012)

69. N. Gisin, G. Ribordy, W. Tittel, H. Zbinden, Rev. Mod. Phys. **74**, 145 (2002)
70. R. Raussendorf, H.J. Briegel, Phys. Rev. Lett. **86**, 5188 (2001)
71. H.J. Briegel, D.E. Browne, W. Dur, R. Raussendorf, M. Van den Nest, Nat. Phys. **5**, 19 (2009)
72. B. Ancochea, A. Bramon, M. Nowakowski, Phys. Rev. D **60**, 094008 (1999)
73. A. Di Domenico et al., Found. Phys. **42**, 778 (2012)
74. U. Singh, M.N. Bera, H.S. Dhar, A.K. Pati, Phys. Rev. A **91**, 052115 (2015)
75. S. Bhattacharya, S. Banerjee, A.K. Pati, Quantum Inf. Process. **17**, 1 (2018)
76. J.R. Ellis, N. Mavromatos, D.V. Nanopoulos, Int. J Mod. Phys. A **13**, 1059 (1998)
77. N.E. Mavromatos, S. Sarkar, Phys. Rev. D **74**, 036007 (2006)